Spring 4-2014

Classifying the Functionality of Primosome Protein A in Deinococcus Radiodurans

Jacob Boone

Classifying the Functionality of Primosome Protein A in *Deinococcus Radiodurans*

Honors Thesis

Jacob Boone

Department: Chemistry

Advisor: Matthew E. Lopper, Ph.D.

April 2014

Classifying the Functionality of Primosome Protein A in *Deinococcus Radiodurans*

Honors Thesis

Jacob Boone

Department: Chemistry

Advisor: Matthew E. Lopper, Ph.D.

April 2014

Abstract

Deinococcus radiodurans is an extremophile bacterium with the capacity to withstand tremendous DNA damage that causes disruption of replisome complex activity. The efficiency of origin-independent replisome reloading directly correlates to effectiveness of DNA damage coping strategies, and remains largely undefined in *D. rad* primosome components. Investigation of *D. rad* PriA as a helicase protein was conducted to determine if PriA could be classified as a fossilized helicase. This project tested the three functions of known helicases by comparing *E. coli* and *D. rad* PriA. DNA binding, DNA unwinding, and ATP hydrolysis assays were performed on both proteins separately and results compared. *E.coli* PriA demonstrated ability to perform all three helicase functions while *D.rad* PriA only demonstrated ability to bind to DNA. The results supported the hypothesis, thus classifying *D.rad* PriA as a fossilized helicase. While the PriA protein of *D.rad* may be structurally similar to PriA proteins in other bacteria, the evolution of the *D. rad* genome over time has rendered the helicase function of *D.rad* PriA inoperable.

Table of Contents

Introduction

In 1956, live specimens of spherical bacteria were isolated from a can of ground meat after gamma-radiation sterilization at 4,000 Gray [4]. The dose was 250 times higher than the normal decontamination dose used to kill *Eschereschia coli*, and 800 times higher than a lethal does of gamma-radiation to humans. Due to observed radiation resistant capabilities, scientist gave the newly discovered bacterium the name *Deinococcus radiodurans*. The *Deinococcus* phylum consists of a group of bacteria possessing great resistance to environmental hazards. Although ionizing gamma-radiation is an almost exclusively artificial DNA damaging process used in laboratories, *D. rad* is no exception to the environmental resistance rule in the *Deinococcus* family [4]. The bacterium is found primarily in arid soil exposed to extreme dehydration, which can cause double strand breaks in chromosomal DNA by oxidizing the phosphodiester backbone of connected nucleotides [5]. The damage imposed by dehydration leaves the cell chromosome in pieces replisome proteins cannot duplicate, thus halting cell replication. Research has observed a remarkable ability *D.rad* possesses of piecing broken chromosomal DNA together utilizing many different repair processes [3]. These DNA repair mechanisms are the first step in achieving renewed cell viability after damage, and are conserved in many bacterial species including *D. rad* [3].

Double stranded DNA damage can be repaired in four different ways in standard model bacteria [3]. *E. coli* is used frequently to describe DNA repair process in bacteria, and has become the standard for defining the homologous recombination model as well as other repair processes. Homologous recombination is a frequently used form of DNA repair, and recruits the RecBCD complex of proteins to create 3’ overhangs on damaged

segments of DNA by helicase and ATP-dependent nuclease function. The RecA protein is loaded by the RecBCD complex on to the single stranded 3' overhangs and helps facilitate the positioning of the overhang segments against a homologous template strand. DNA polymerase I extends the 3' overhang segments by replication using the template strand. DNA ligase attaches the extended overhang to the undamaged DNA and a crossover event attaches the template DNA to the originally damaged DNA strand. Two undamaged, double stranded DNA segments result allowing the cell to return to normal function [3].

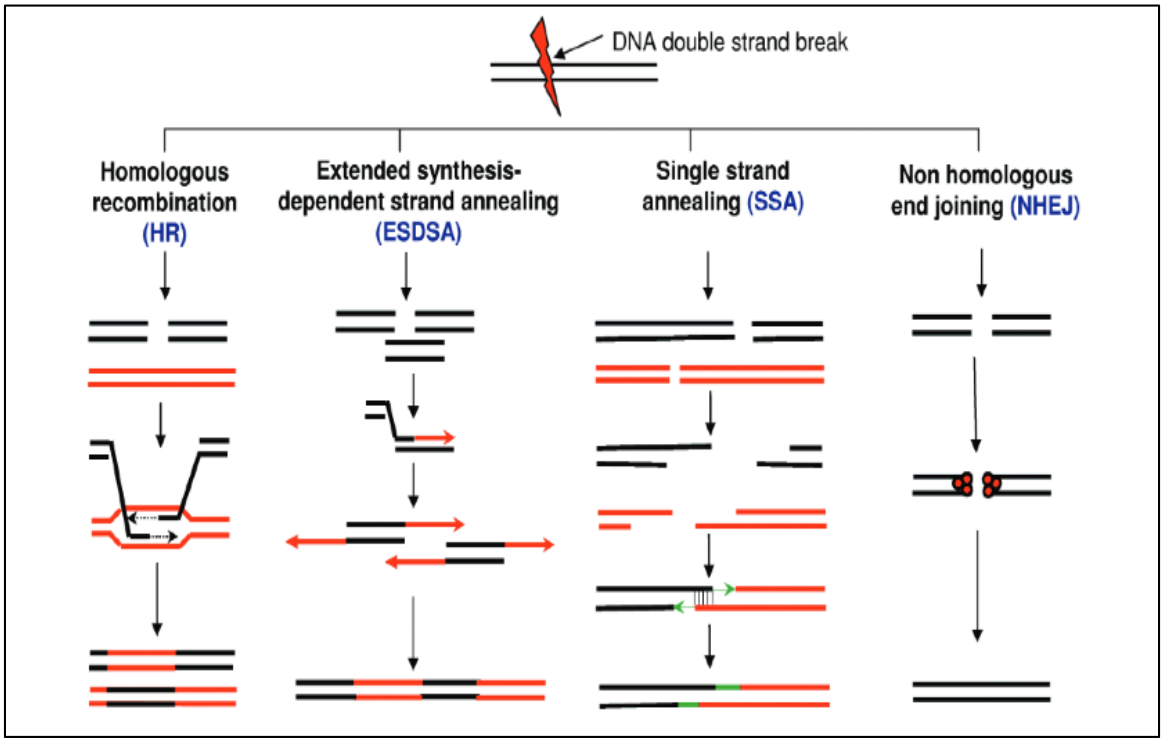

FIGURE 1. **Different proposed pathways of double stranded DNA break repair in *Deinococcus Radiodurans*** (Blasius *et al.*, 2008)

Two other repair processes utilized by bacterial species occur earlier in radiation and may serve as an initial mechanism to set up more complex RecBCD double strand repair. Single Strand Annealing (SSA) and Extended Synthesis-Dependent Strand Annealing (ESDSA) are RecA independent repair pathways able to use single stranded 3'

overhangs to connect two damage DNA segments. The SSA mechanism recruits nuclease enzymes to damaged, homologous chromosomes and creates 3' overhang segments at the double strand break sight. Homologous segments of DNA are joined together and polymerase enzymes fill in gaps lacking nucleotides [3]. The ESDSA mechanism joins single strands in the same way, but creates 3' overhangs by extension using undamaged portions of overall damaged, homologous strands instead of degradation in a 3' to 5' direction [3].

D. rad uses a variation of homologous recombination, conserved SSA and ESDSA mechanisms, and a process used mainly in eukaryotes called nonhomologous end joining (NHEJ) to repair double strand breaks [3]. The variation in *D. rad* homologous recombination lies in variation of protein components accomplishing the same task as the RecBCD complex. *D. rad* utilizes a RecFOR complex of proteins instead to load RecA on to single strand overhangs [14]. Other bacteria utilizing the RecFOR pathway show greater multiplicity of function between proteins, and experimental evidence suggests the same in *D. rad* [3]. NHEJ has not been experimentally observed in *D. rad*, but the bacterium shares many common proteins with eukaryotic cells possessing the ability to perform NHEJ suggesting the mechanism is occurring [3]. In particular, the PprA protein is believed to play a major role in *D. rad* NHEJ as the protein displays the ability to bind to DNA containing double strand breaks, inhibit nuclease activity, and stimulate DNA end joining reactions catalyzed by ATP or NADH dependent DNA ligases [3]. The combination and efficiency of these DNA repair mechanisms in *D. rad* contribute to the capability of the bacterium to survive in such extreme situations.

While all cells have developed pathways to cope with double stranded DNA damage, the cell does not achieve normal function again until DNA replication pathways can be restored [6]. DNA replication pathways in bacteria are highly conserved processeses that starts at a segment of DNA called the *oriC* sequence. The *oriC* nucleotides provide a binding site for bacterial DnaA proteins, which create single stranded DNA necessary for binding of DnaB [11]. DnaA loads the DnaB protein on to DNA by way of a DnaC/DnaB complex, and eventually dissociates from DNA leaving the DnaB replicative helicase bound to each of two single strands (see Figure 2). The replisome complex of proteins binds to DNA behind DnaB and begins replication using single stranded templates created by DnaB helicase activity [11]. Under normal conditions, the bacterial replisome will complete a full copy of the double stranded genome and the replisome will detach from the DNA [11]. However, when double strand DNA damage occurs DnaB and the replisome complex fall off the DNA strand leaving behind a partially replicated bacterial genome. At this time, the DNA repair processes previously mentioned repair double stranded breaks, creating a structure called a replication fork (seen in Figure 2) at the site of replisome malfunction [11]. In standard bacterial models, a set of primosome proteins is utilized to reload DnaB on to the replication fork so the replication process can be completed [15]. In *E. coli*, PriA first binds to DNA and uses an ATP-dependent helicase domain to unwind 15-20 nucleotides in a 3' to 5' direction. The PriB and DnaT proteins bind to PriA in succession creating a protein complex, then load the DnaC/DnaB complex on to the newly created primosome complex. The protein complex dissociates from the replication fork after DnaB is loaded on to single stranded DNA, and DnaB is left to perform helicase function in the 5' to 3'

direction on the rest of the bacterial genome [11]. This efficiency of origin-independent replisome reloading directly correlates to the amount of double strand DNA damage a cell can cope with while still remaining viable.

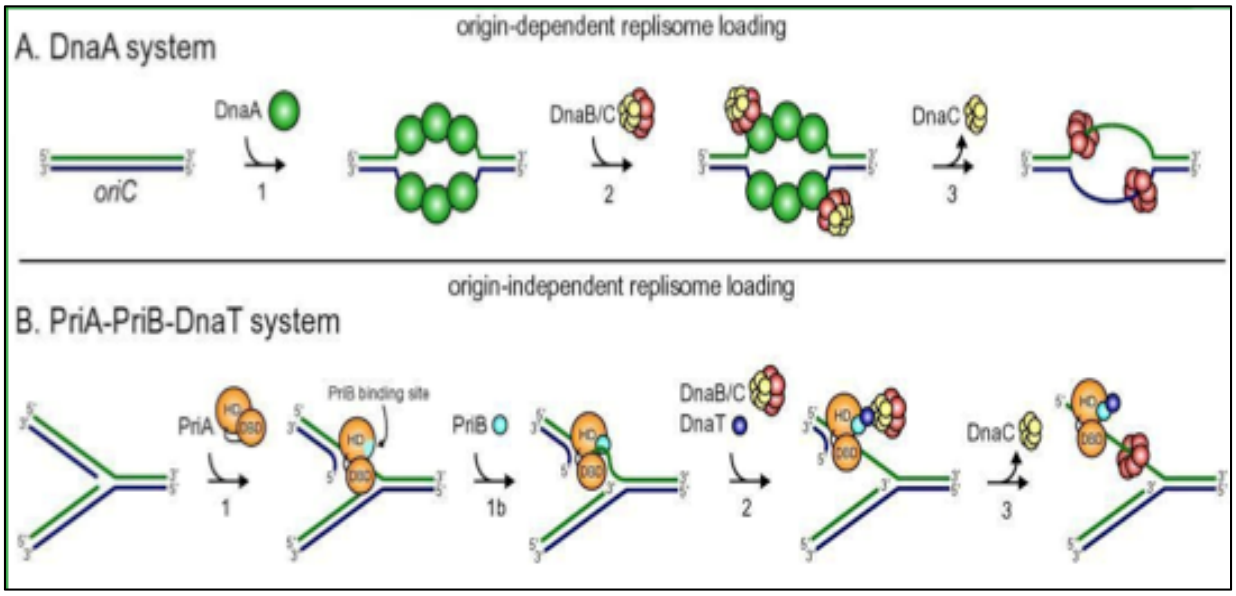

FIGURE 2. **Origin-dependent and origin-independent replisome reloading in standard bacteria models**. (Lopper, 2013)

D. rad displays some variation in the components making up the PriA system, but unlike the homologous recombination pathway, origin-independent replisome reloading remains largely undefined in the bacterium. Upon direct comparison with standard bacteria models, specifically *E. coli*, many of the components of the PriA system in *D. rad* are missing. *D.rad* codes for PriA and DnaB proteins, indicating a probable use of a similar PriA system. However, *D. rad* does not code for PriB, DnaT, or DnaC proteins proven to have great effect on *E. coli* viability [9]. Upon further examination of the *D. rad* PriA primary sequence, the protein displays an extended N-terminus of about 250 amino acids when compared to PriA proteins contained in other bacterial species

(comparison shown in Figure 3). These observations of the *D. rad* primosome system may have two implications. If PriA plays a role similar to that of *E. coli* PriA in loading DnaB on to replication forks, the *D. rad* PriA would display characteristics of a helicase by binding to DNA and hydrolyzing ATP to unwind DNA. The variation in primary structure caused by mutations over time may have caused the PriA protein to gain a greater efficiency in loading DnaB on to stalled replication forks giving rise to an increase in resistance to DNA damaging environments. By contrast, the variation in the primosome system may have resulted in a loss of function, in which case *D. rad* PriA would not display ATP-dependent helicase function. In the case of loss of function due to mutations in the segments of the genome coding for PriA over time, the PriA protein in *D. rad* could be classified as a fossilized helicase.

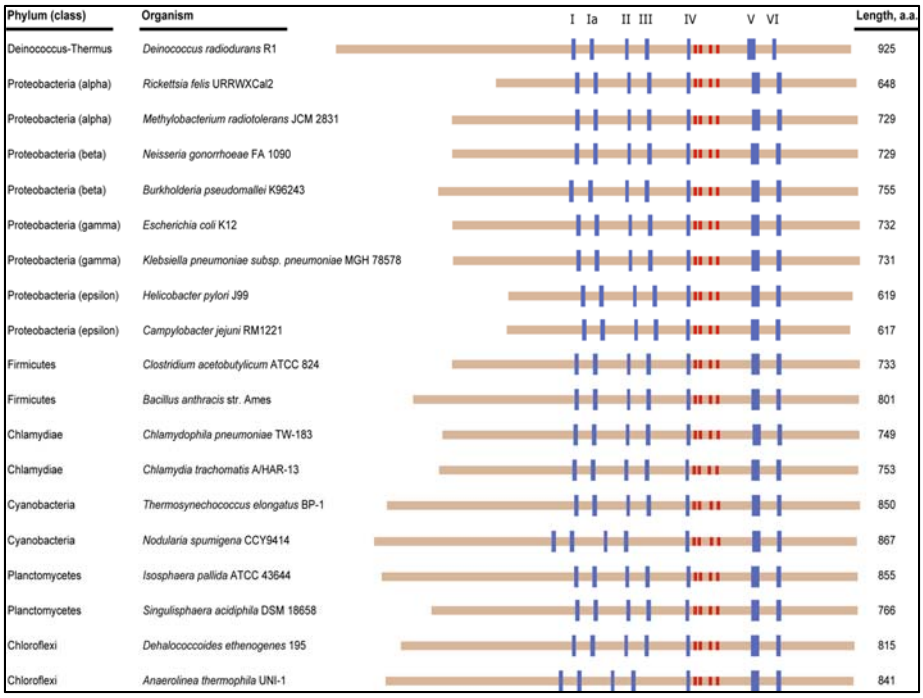

FIGURE 3. **Comparison of PriA primary structure in relevant bacterial species.** (Lopper, 2013)

Methods and Materials

Amplification of D. rad and E. coli PriA

D. rad PriA was purified from the ML300 strain *E. coli* containing the pET28b: *D.rad*-PriA plasmid. Cells were grown in Luria Bertani medium containing 375 ug/mL of kanamycin and 375 ug/mL of chloramphenicol at 37 ^{o}C and 180 rpm until an OD_{600} of 0.84 was reached. Expression of *D. rad* PriA was induced using 0.5 mM of IPTG and cell cultures were incubated at 37 ^{o}C an 180 rpm for 4 hours. Cells were collected by centrifugation at 4^{o}C and 3716 x g. Collected cells were lysed in lysis buffer containing 10 mM tris-HCl pH 8.5, 0.5 M NaCl, 10 mM imidazol, 1 mM β-mercaptoethanol, 10% glycerol (v/v), 1 mM phenylmethylsulfonyl fluoride (PMSF). After lysis buffer was introduced, the lysate was sonicated at 5 x 30 second pulse bursts and 70% power. The lysate was clarified by centrifugation at 40,000 x g and 4^{o}C for 25 minutes and supernatant collected. His-tagged PriA in the lysate was bound to nickel-NTA agarose (Qiagen) and incubated at 4^{o}C with gentle rocking. The nickel-NTA agarose/lysate slurry was placed through a fine filter column and supernatant drained off. Nickel-NTA agarase beads were washed with 10 column volumes of buffer containing 10 mM tris-HCl pH 8.5, 10% glycerol (v/v), 0.5 M NaCl, 10 mM imidazole, and 1 mM β-mercaptoethanol. His-tagged PriA bound to the nickel-NTA agarose beads were eluted in buffer solution containing 10 mM tris-HCl pH 8.5, 100 mM NaCl, 250 mM imidazol, 1 mM β-mercaptoethanol, and 10% glycerol (v/v). The nickel-NTA agarose eluate was incubated with 1 unit/uL Thrombin and was dialyzed against a dialysis buffer containing 10 mM tris-HCl, 100 mM NaCl, 1 mM β-mercaptoethanol, and 10% glycerol (v/v) at 4^{o}C. The dialyzed eluate was centrifuged at 4^{o}C and 3716 x g for 10 minutes and loaded

on to a QFF ion exchange column pre-equilibrated with QFF Buffer A containing 10 mM tris-HCl pH 8.5, 10% glycerol (v/v), 100 mM NaCl, and 1mM β-mercaptoethanol. The dialyzed eluate was resolved through the column at 0.5 L/min using a 10 column volume linear gradient of 0%-100% QFF Buffer B containing 10 mM tris-HCl pH 8.5, 10% glycerol (v/v), 1 M NaCl, and 1mM β -mercaptoetanol. Fractions 30, 31, 32, and 33 were pooled and concentrated using a Centriprep Ultracel YM-3 (Millipore) concentrator and centrifugation at 2643 x g and 4ºC for 3 hours. The concentrated protein solution was collected and loaded on to an S300 size-exclusion column pre-equilibrated with S300 buffer containing 10 mM tris-HCl pH 8.5, 10% glycerol (v/v), 500 mM NaCl, and 1mM β-mercaptoethanol. The concentrated protein solution was resolved through the column at 0.5 mL/min using two column volumes of previously defined S300 buffer. Fractions 18, 19, 20, and 21 were pooled and concentrated using an Amicon Ultra 3K MNCO (Millipore) concentrator and centrifugation at 2643 x g and 4ºC for 4 hours. Concentrated *D. rad* PriA protein solution was stored at -80ºC.

E. coli PriA was purified from the ML104 *E. coli* strain containing the pET28b: *Ec*-PriA plasmid. Cells were grown in Luria Bertani medium containing 375 ug/mL of kanamycin and 375 ug/mL of chloramphenicol at 37 ºC and 180 rpm until an OD_{600} of 0.96 was reached. Expression of *E. coli* PriA was induced using 0.5 mM of IPTG and cell cultures were incubated at 37 ºC and 180 rpm for 4 hours. Cells were collected by centrifugation at 4ºC and 3716 x g. Collected cells were lysed in lysis buffer containing 10 mM hepes pH 7, 0.5 M NaCl, 10 mM imidazol, 1 mM β-mercaptoethanol, 10% glycerol (v/v), 1 mM PMSF. After lysis buffer was introduced, the lysate was sonicated at 5 x 30 second pulse bursts and 70% power. The lysate was clarified by centrifugation

at 40,000 x g and 4ºC for 25 minutes and supernatant collected. His-tagged PriA in lysate was bound to nickel-NTA agarose (Qiagen) and incubated at 4ºC with gentle rocking. The nickel-NTA agarose/lysate slurry was placed through a fine filter column and supernatant drained off. Nickel-NTA agarase beads were washed with 10 column volumes of buffer containing 10 mM Tris-HCl hepes pH 7, 10% glycerol (v/v), 0.5 M NaCl, 10 mM imidazole, and 1 mM β-mercaptoethanol. His-tagged PriA bound to the nickel-NTA agarose beads were eluted in buffer solution containing 10 mM hepes pH 7, 100 mM NaCl, 250 mM imidazol, 1 mM β-mercaptoethanol, and 10% glycerol (v/v). The nickel-NTA agarose eluate was incubated with 1 unit/uL thrombin and was dialyzed against a dialysis buffer containing 10 mM hepes pH 7, 100 mM NaCl, 1 mM β-mercaptoethanol, and 10% glycerol (v/v) at 4ºC. The dialyzed eluate was centrifuged at 4ºC and 3716 x g for 10 minutes and loaded on to a SPFF ion exchange column pre-equilibrated with SPFF Buffer A containing 10 mM MES pH 6, 10% glycerol (v/v), 100 mM NaCl, and 1mM β-mercaptoethanol. The dialyzed eluate was resolved through the column at 0.5 L/min using a 10 column volume linear gradient of 0%-100% SPFF Buffer B containing 10 mM MES pH 6, 10% glycerol (v/v), 1 M NaCl, and 1mM β-mercaptoethanol. Fractions 1, 2, 3, 4, 5, and 6 were pooled and concentrated using a Centriprep Ultracel YM-3 (Millipore) concentrator and centrifugation at 2643 x g and 4ºC for 3 hours. The concentrated protein solution was collected and loaded on to an S300 size-exclusion column pre-equilibrated with S300 buffer containing 10 mM MES pH 6, 10% glycerol (v/v), 500 mM NaCl, and 1mM β-mercaptoethanol. The concentrated protein solution was resolved through the column at 0.5 mL/min using two column volumes of previously defined S300 buffer. Fractions 22, 23, 24, and 25 were

pooled and concentrated using an Amican Ultra 3K MNCO (Millipore) concentrator and centrifugation at 2643 x g and 4ºC for 4 hours. Concentrated *D. rad* PriA protein solution was stored at -80ºC.

Protein Concentration and Purity Determined

UV-Vis spectroscopy was used to determine the concentration of both purified PriA protein solutions. Six samples containing 5 µL of *D. rad* PriA solution and 145 µL of 8 M Guanidine-HCl were made and absorbance units measured at wavelength 280 nm. Before each reading, the UV-Vis spectrophotometer was blanked using a sample contaning 145 µL of 8 M Guanidine-HCl and 5 µL of S300 buffer consisting of 10 mM tris-HCl pH 8.5, 10% glycerol (v/v), 500 mM NaCl, and 1mM β-mercaptoethanol. Six absorbance readings were averaged and the Lambert-Beer law was used to determine concentration of the *D. rad* PriA protein solution after accounting for the dilution of each samples. In the Lambert-Beer calculation, the molar extinction coefficient 184, 370 $M^{-1}cm^{-1}$ and path length of 1 cm was used. Six samples containing 5 µL of *E. coli* PriA solution and 145 µL of 8 M Guanidine-HCl were made and absorbance units measured at wavelength 280 nm. Before each reading, the UV-Vis spectrophotometer was blanked using a sample contaning 145 µL of 8 M Guanidine-HCl and 5 µL of S300 buffer consisting of 10 mM MES pH 6, 10% glycerol (v/v), 500 mM NaCl, and 1mM β-mercaptoethanol. Six absorbance readings were averaged and the Lambert-Beer law was used to determine concentration of the *D. rad* PriA protein solution after accounting for the half dilution of each sample. In the Lambert-Beer calculation, a molar extinction coefficient of 105, 870 $M^{-1}cm^{-1}$ and path length of 1 cm was used.

Protein purity was determined using SDS-page gel electrophoresis at 130 volts over 90 minutes. Both *D. rad* and *E. coli* PriA purity were determined by the same procedure but were examined using separate gels. Six solutions were made up according to the Table 1 and 15 µL of each solution was loaded on to the polyacrylamide gel. The 1.0 µL lane of the final PriA solution was used to correspond to a 10 % impurity in the 10.0 µL solution while the 0.1 µL lane was used to correspond to a 1% impurity in the 10.0 µL solution. Results can be seen in Table 2.

TABLE 2. **Contents of Solutions Loaded on to Polyacrylamide Gels**

Label	**Amount of Final Protein Solution**	**Milli-Q H_2O**	**Sample Buffer**
0.1 µL of Final *D. rad* PriA Solution	1 µL of a 1/10 dilution of final protein product	19 µL	5 µL
1.0 µL of Final *D. rad* PriA Solution	1 µL	19 µL	5 µL
10 µL of Final *D. rad* PriA Solution	10 µL	10 µL	5 µL
0.1 µL of Final *E. coli* PriA Solution	1 µL of a 1/10 dilution of final protein product	19 µL	5 µL
1.0 µL of Final *E. coli* PriA Solution	1 µL	19 µL	5 µL
10 µL of Final *E. coli* PriA Solution	10 µL	10 µL	5 µL

TABLE 3. **Final protein solution concentration and purity**

Strain	**Concentration (µM)**	**Purity**
E. coli PriA	50.16	98%
D. rad PriA	26.00	90%

PriA Protein Binding Assays

All binding assays were performed using fluorescence polarization spectroscopy at 25^{o}C with a Beacon 200 fluorescence polarization system (Invitrogen). *D. rad* and *E. coli* PriA proteins were analyzed using the same procedure. PriA proteins were diluted

serially from 2250 nM to 0.01 nM in FP buffer containing 20 mM tris-HCl pH 8.0, 10% glycerol (v/v), 50 mM NaCl, 1 mM β-mercaptoethanol, 0.1 g/L Bovine Serum Albumin (BSA). The dilutions were incubated with 1 nM 3' – fluorescein labeled ssDNA oligonucleotide of 15-mer (5' – TAG CCA TGT AAT CGT) length in a total volume of 100 μL. Apparent dissociation constants were calculated by determining the concentration of PriA needed to bind to half of the 15-mer oligonucleotide. The unbound state is reported by the fluorescence polarization of the fluorescein labeled ssDNA in the absence of PriA. The fully bound state is reported as the fluorescence polarization reading of the fluorescein labeled ssDNA in the presence of a concentration of PriA large enough to saturate the fluorescence polarization reading [16].

PriA Protein Helicase Assays

All DNA unwinding Assays were performed using fluorescence polarization spectroscopy at 25°C with a Beacon 2000 fluorescence polarization system (Invitrogen). *D. rad* and *E. coli* PriA proteins were analyzed using the same procedure. PriA proteins were diluted serially from 50 nM to 0.25 nM in Helicase Buffer containing 20 mM tris HCl pH 8, 50 mM NaCl, 3 mM $MgCl_2$, and 1 mM β-mercaptoethanol. The dilutions were incubated with a 1:40 dilution of DNA forks of varying lengths (structure and length can be seen in Table 4) in a total volume of 100 μL. After incubation with the fork, 10 μL of 10 mM adenosine triphosphate (ATP) was added and each solution was incubated at 37°C for 10 minutes. 10 μL of SDS detergent was added, 100 μL of each solution was placed in separate tubes, and polarization readings were taken. Samples were then incubated at 95°C for 20 seconds, placed on ice for 10 seconds, and polarization readings were taken. This procedure was repeated for a separate, duplicate

experiment measuring helicase assay solutions of 0 nM *D. rad* PriA, 10 nM *D. rad* PriA, and 10 nM *D. rad* PriA with 1 mM ATP. Fraction unwound values were calculated by determining the concentration of PriA needed to unwind the entirety of fork DNA in solution using the heated sample polarization readings to represent complete detachment of the fluorescein labeled ssDNA (oML 277 and oML 288) from the DNA fork. The intact DNA fork state is reported as a fraction unwound of 0% while the degree of fluorescein labeled ssDNA segment detachment is reported as an increase in the percent of fraction unwound.

TABLE 4. **Structure of oligonucleotide DNA fork substrates.** (Lopper, 2013)

Fork 1	DNA Sequence	Fork 2	DNA Sequence
oML 211	GTCGGATCCTCTAGA CAGCTCCATGATCAC TGGCACTGGTAGAAT TCGGC	oML 211	GTCGGATCCTCTAG ACAGCTCCATGATC ACTGGCACTGGTAG AATTCGGC
oML 287	ACGATTACATTGCTA CATGGAGCTGTCTAG AGGATCCGAC	oML 276	AACGTCATAGACGA TTACATTGCTACAT GGAGCTGTCTAGAG GATCCGAC
oML 212	GCCGAATTCTACCAG TGCCAGTGAT	oML 212	GCCGAATTCTACCA GTGCCAGTGAT
oML 288	TAGCAATGTAATCGT	oML 277	TAGCAATGTAATCG TCTATGACGTT
			

PriA ATPase Assays

All ATPase assays were performed using UV-Vis spectroscopy monitoring absorbance readings at wavelength 340 nm every 1 second over a 300 second interval at 37°C. This assay used an ATP regeneration system that converts ADP to ATP in a

reaction that is coupled to the conversion of NADH to NAD^+ (seen in Figure 4). The coupled reaction was monitored by measuring the decrease in absorbance at 340 nm due to NADH oxidation using spectrophotemetry. *D. rad* and *E.coli* PriA ATPase assays were performed by the same procedure. PriA proteins were diluted to separate concentrated solutions of 100 nM, 50 nM 25 nM, 10 nM, and 1 nM. PriA protein solutions were diluted in 20 mM hepes pH 8, 50 mM NaCl, 2 mM $MgCl_2$, 7 mM β-mercaptoethanol, 0.1 g/L BSA, 2 mM PEP, 0.1 mM NADH, 1.8-3 units pyruvate kinase/lactate dehydrogenase (PK/LDH) mixture, and 1 μM dT_{36} thymidine oligonucleotide. Each solution was placed in a quartz cuvet and 10 μL of 10 mM ATP (Final concentration 1 mM) was added immediately before absorbance readings were taken. Steady state Δ[NADH]/Δt rates were calculated using the molar extinction coefficient of 6220 $M^{-1}cm^{-1}$ for NADH and are equivalent to Δ[ATP]/Δt. The kinetic value V_o was determined by fitting the rates of ATP hydrolysis from individual experiments to the Michaelis-Menten equation for which PriA was varied [16].

$$V_o = \frac{V_{max}[PriA]}{K_m + [PriA]}$$

A spike experiment was conducted to examine the affects of adding *E. coli* PriA to a solution containing *D. rad* PriA after a 300 second interval. A *D. rad* PriA ATPase assay was performed as described using 100 nM final PriA concentration. After the 300 second interval of measuring NADH consumption, *E. coli* PriA protein was added to give a final concentration of 100 nM in the *D. rad* PriA ATPase assay solution and NADH consumption was measured as described for another 300 seconds. Steady state Δ[NADH]/Δt rates were calculated before and after the spike as the previously described ATPase procedure.

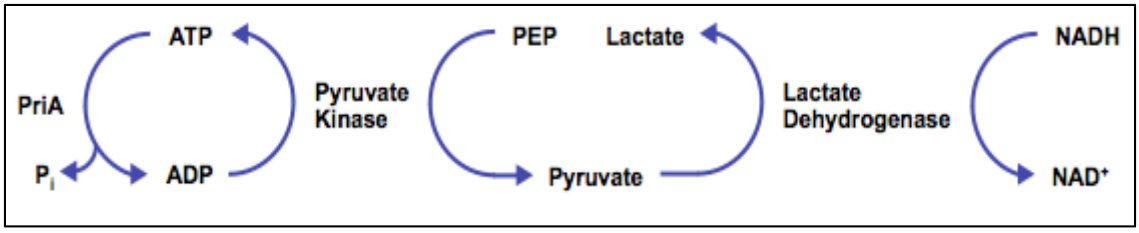

FIGURE 4. **ATP Regeneration system used to investigate ATPase activity in PriA proteins.** (Lopper, 2013)

Results and Discussion

D. rad PriA displays comparable DNA binding ability to E. coli PriA

All binding assays were conducted using fluorescence polarization spectroscopy to examine the physical interaction between *D. rad* PriA or *E. coli* PriA and a 15-mer oligonucleotide (5' – TAG CCA TGT AAT CGT) of single stranded DNA with a 3' fluorescein tag. The presence of the 3' fluorescein tag allowed PriA binding to be measured by an increase in fluorescence polarization of the PriA:DNA complex relative to the unbound DNA [8]. PriA protein was serially diluted, incubated with 1 nM fluorescein labeled DNA, and the fluorescence polarization was measured. Experimental dissociation constants were obtained by determining the concentration of PriA needed to achieve 50% binding to the ssDNA substrate.

Both *D. rad* and *E. coli* PriA displayed capacity to bind to the ssDNA. The apparent dissociation constant calculated for *D. rad* PriA was 215 ± 17 nM. *E. coli* PriA displayed a higher affinity to bind to DNA as the apparent dissociation constant calculated was 125 ± 13 nM. Although *E. coli* PriA has a higher binding affinity, both proteins display a capability to bind to DNA suggesting the binding site of *D. rad* PriA has not evolved to serve a different function. *D. rad* PriA displays binding capabilities to single stranded DNA independent of other proteins similar to *E. coli* PriA, although the

effect of *D. rad* DnaB or other proteins on binding affinity was not tested and remains unknown.

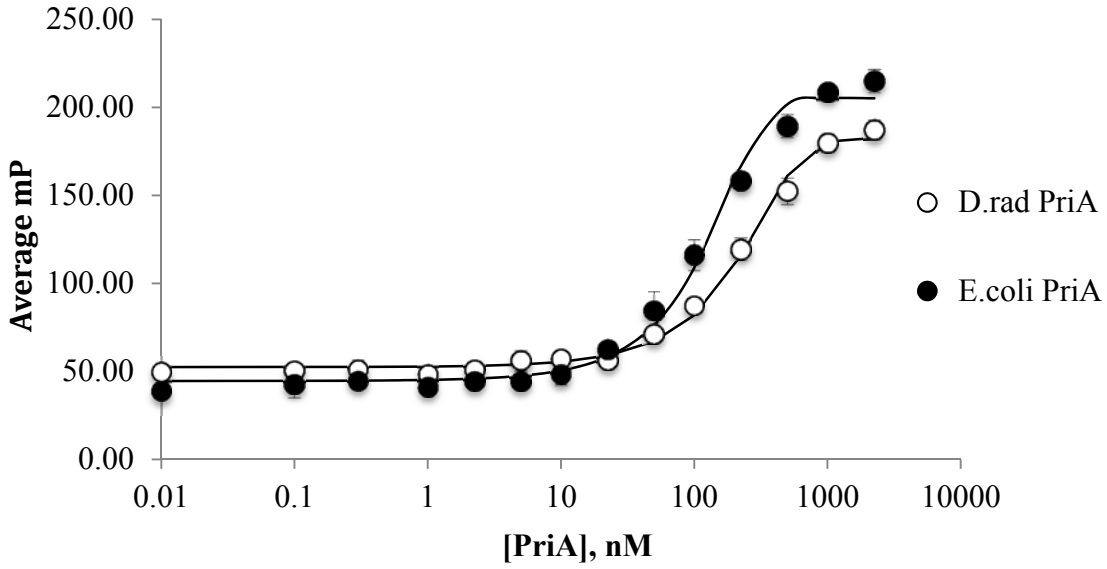

FIGURE 5. **DNA binding activity in *D. rad* and *E. coli* PriA.** PriA was serially diluted and incubated with 1 nM fluorescein labeled ssDNA. Measurements are reported in triplicate and error bars represent one standard deviation from the

D. rad does not display helicase activity when bound to a replication fork

To test whether or not *D. rad* PriA had functional capabilities after binding to DNA, helicase activity of *D. rad* PriA was tested. Two fluorescently labeled DNA fork substrates, labeled Fork 1 and Fork 2, were used in the helicase assays. Each fork was comprised of four oligonucleotides (specific sequences seen in Table 2), and the 3' fluorescein labeled DNA had a significantly smaller molecular weight than the molecular weight of the combined fork. The relative size difference between combined oligonucleotides allowed unwinding of the fork substrate to be measured by decrease in polarization as a result of dissociation of the labeled DNA from the reminder of the intact fork [16]. PriA protein was incubated with Fork 1 or Fork 2 and ATP. Fluorescence polarization spectroscopy was used to measure the degree of DNA unwinding caused by

PriA helicase activity. Polarization readings were used to find the percent of fork DNA substrate in solution that had been unwound as the quantity Fraction Unwound (%).

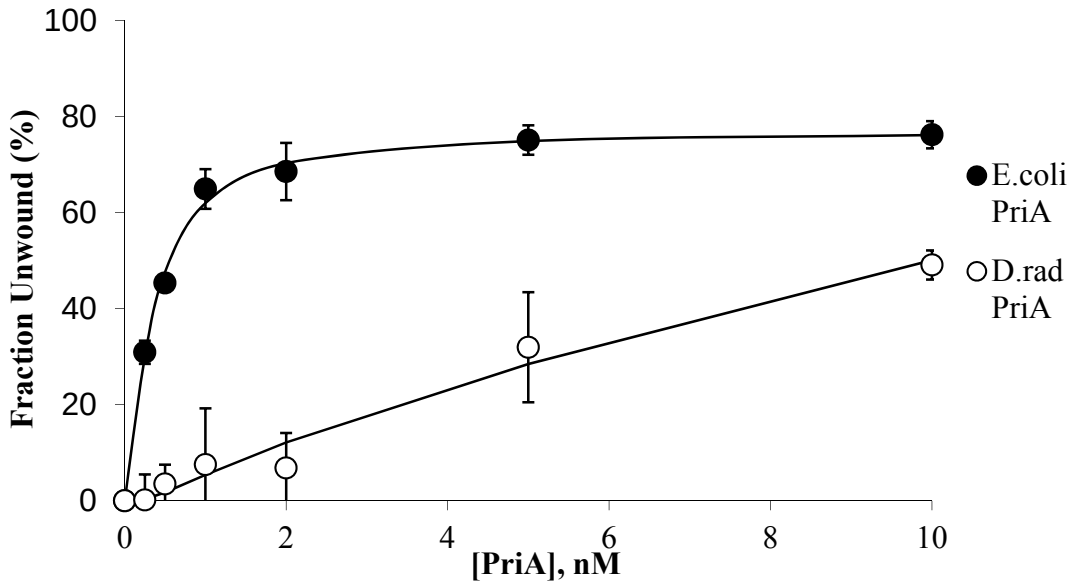

FIGURE 6. **Helicase activity of *D. rad* and *E. coli* PriA.** Serially diluted PriA was incubated with 1:40 dilution Fork 1 duplex DNA substrate (Table 2) with 3' fluorescein labeled oligonucleotide segment and 1 mM ATP. Measurements are reported in triplicate and and error bars represent one standard deviation from the mean.

Solution Label	[PriA], nM	[ATP], mM	Fraction Unwound Trial 1 (%)	Fraction Unwound Trial 2 (%)
0	0	1	0	0
10	10	0	51	40
10 w/ ATP	10	1	73	55

TABLE 5. ***D. rad* PriA helicase activity with and without ATP in the presence of Fork 1**. 0 and 10 nM *D. rad* PriA was incubated with 1:40 dilution Fork 2 duplex DNA substrate (Table 2) with 3' fluorescein labeled oligonucleotide segment and 1 mM ATP where indicated. Trial measurements are reported in duplicate.

Comparison to *E. coli* PriA helicase activity shows an absence of DNA unwinding capability in *D. rad* PriA. Comparison of the trends observed in both *E. coli* and *D. rad* PriA helicase assays using the fork 2 DNA substrate and ATP indicate an

absence of ATP dependent helicase capability in *D. rad* PriA. Despite an increase in concentration of *D.* rad PriA protein, no significant increase in fraction of DNA unwound was observed in comparison to helicase assays performed using *E. coli* PriA. While the helicase assays performed with Fork 1 display trends consistent with fork unwinding in *D. rad* PriA, the trends were likely the result of disruption of weak interactions between nucleotide bases due to conformational changes during formation of the PriA:DNA complex. The result of helicase assays performed using Fork 1 without ATP produced similar fraction unwound values (Average fraction unwound without ATP = 45% and average fraction unwound with ATP = 65%) suggesting any unwinding taking place is ATP independent. Furthermore, helicase assays performed using Fork 2 and ATP produce trends in *D. rad* PriA consistent with no unwinding of the DNA fork substrate. These results compared with results using Fork 1 substrate suggest elongation of the 3' fluorescein labeled oligonucleotide eliminate any significant unwinding potential due to conformational changes in the PriA DNA binding site.

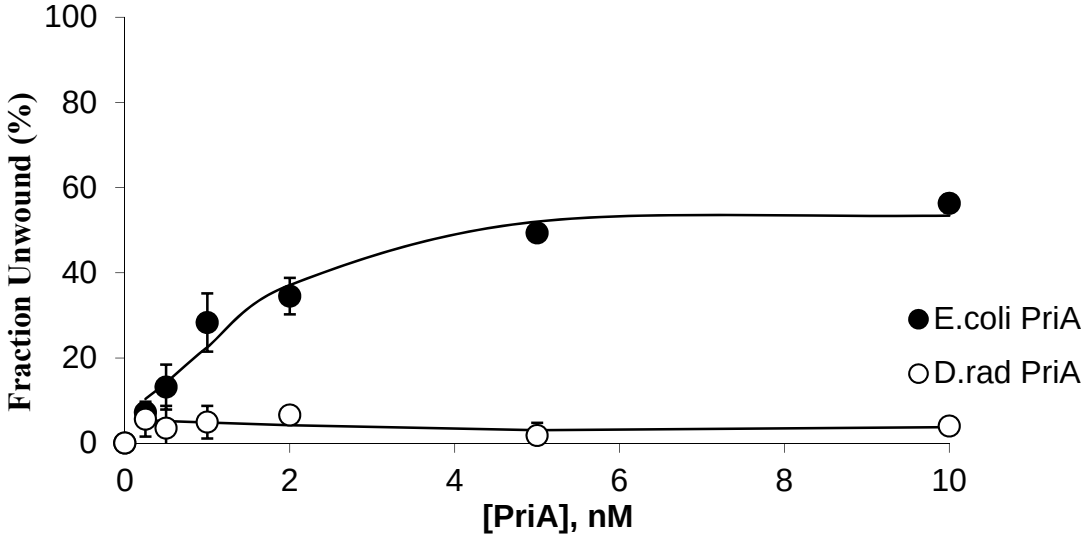

FIGURE 7. **Helicase activity of *D. rad* and *E. coli* PriA.** Serially diluted PriA was incubated with 1:40 dilution Fork 2 duplex DNA substrate (Table 2) with 3' fluorescein labeled oligonucleotide segment and 1 mM ATP. Measurements are reported in triplicate and and error bars represent one standard deviation from the mean.

D. rad PriA does not exhibit ability to hydrolyze ATP

ATPase function in *E. coli* and *D. rad* PriA was tested using an ATP regeneration system leading the oxidation of NADH. PriA was incubated with ATP, NADH, dT_{36} oligonucleotide, and other biochemical components necessary for NADH oxidation outlined in Figure 7. Degradation of NADH absorbance at 340 nm was measured over a 300 second interval. Steady state $\Delta[NADH]/\Delta t$ rates were calculated correlating directly with $\Delta[ATP]/\Delta t$. Steady state rates were applied to the Michaelis-Menten relationship described previously and kinetic value V_o was calculated [16].

D. rad PriA ATPase assay comparisons with *E. coli* PriA revealed no significant ATPase capability. *E. coli* PriA exhibited an increase in ATP consumption per second as concentration was increased while an increase in *D. rad* PriA concentration had no noticeable affect on ATP consumption rate. In addition, the spike experiment produced a V_o value of 0.7 nM/sec before *E. coli* PriA was added to the *D. rad* PriA helicase assay solution, and a value of 191.3 nM/sec after addition of *E. coli* PriA. These results indicate the presence of some amount of ATP present and used as substrate by *E. coli* PriA in the *D. rad* PriA helicase assay solution after the initial measurement interval of 300 seconds. The presence of ATP in the spike experiment coupled with the observation of insignificant ATP consumption by *D. rad* PriA in the helicase assays suggests a lack of ability for *D. rad* PriA to hydrolyze ATP. Any hydrolyzing activity observed, even if negligible, can most likely be attributed to impurities in the protein solution. The ATP hydrolysis domain may be altered or changed as a result of the extended N-terminus of the protein, resulting in loss of hydrolysis function. However, no concrete conclusion about the hydrolysis domain can be assumed until a three-dimensional crystal structure of

the *D. rad* PriA protein is created and examined.

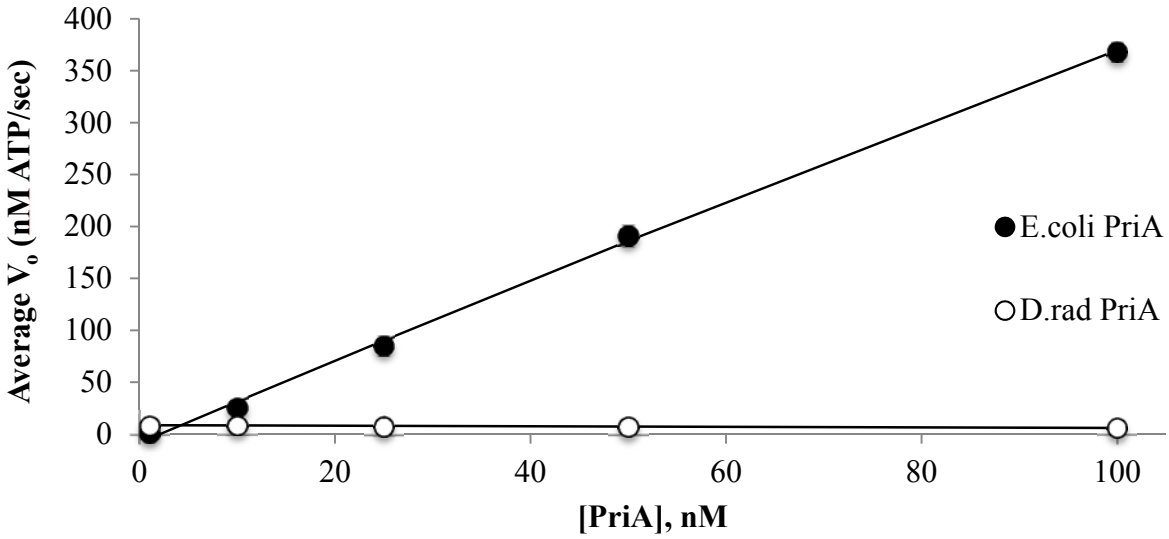

Figure 8. **ATPase activity of *D. rad* and *E. coli* PriA.** Varying concentrations of PriA were incubated with ATP, NADH, and other biochemical agents needed for the ATP regeneration system (Figure 6) and ATP consumption rates calculated. Measurements are reported in triplicate and error bars represent one standard deviation from the mean.

Helicase function no longer exists in D. rad PriA

When compared with the known helicase *E. coli* PriA, *D. rad* PriA does not exhibit hallmark characteristics of a helicase protein by unwinding DNA via ATP hydrolysis, thus differing in function from homologous PriA proteins. The ability for *D. rad* PriA to bind to DNA with affinity comparable to *E. coli* PriA suggests the function of DNA binding has been a conserved function of the protein over time. *D. rad* PriA may very well still serve a primosome role because of the conserved DNA binding function, but the helicase role has been lost over time. Examination of the primary structure of *D. rad* PriA against other homologous PriA proteins (shown in Figure 3) reveals many motif locations and sequences have been conserved, including the ATP hydrolyses domain used in homologous PriA proteins to fuel helicase function. However, the results of the

ATPase and helicase assays coupled with the presence of an extended N-Terminus of *D. rad* PriA suggest a possible correlation between altered protein structure and change in function. The cellular stress of severe dehydration present in the environment of *D. rad* may have propagated mutations in the gene encoding for the PriA protein causing a loss in ATP dependent helicase activity. The negative results of the DNA unwinding and ATPase assays demonstrate loss of helicase function in *D. rad* PriA, while the presence of binding ability demonstrates a retention of one aspect of primosome protein function possessed by a common ancestor of *E. coli* and *D. rad*. The *D. rad* PriA can therefore be classified as a fossilized helicase, having lost helicase function in the PriA protein due to time. While the role *D.rad* PriA plays in origin-independent replication restart still remains unknown, studies of protein-protein interactions with DnaB and creation of a three-dimensional structure of PriA will provide a more detailed look at what domain structures have changed and how the PriA protein function may be affected by domain changes.

Acknowledgements

These studies were supported by funds and grants from the University of Dayton Honors Department and Chemistry Department. I thank Dr. Matthew E. Lopper for designing experimental theory and design for this project. I also thank Danielle Gerbic and Michael Ryan for their collaboration and insightful comments throughout the project.

References

1) Battista, John R. "Against All Odds: The Survival Strategies of Deinococcus Radiodurans." *Annual Review of Microbiology* 51 (1997): 203-24. Print.

2) Berg, Linda, and Matthew E. Lopper. "The PriB Gene of Klebsiella Pneumoniae Encodes a 104-Amino Acid Protein That Is Similar in Structure and Function to Escherichia Coli PriB." Ed. Arthur J. Lustig. *PLoS ONE* 6.9 (2011): E24494. Print.

3) Blassius, Melanie, Ulrich Hubscher, and Suzanne Sommer. "Deinococcus Radiodurans: What Belongs in the Survival Kit?" *Critical Reviews in Biochemistry and Microbiology* 43 (2008): 221-38. Print.

4) Cox, Michael M., and John R. Battista. "Deinococcus Radiodurans — the Consummate Survivor." *Nature Reviews Microbiology* 3.11 (2005): 882-92. Print.

5) Cox, Michael M., James L. Keck, and John R. Battista. "Rising from the Ashes: DNA Repair in Deinococcus Radiodurans." Ed. Susan M. Rosenberg. *PLoS Genetics* 6.1 (2010): E1000815. Print.

6) Cox, Michael M., Myron F. Goodman, Kenneth N. Kreuzer, David J. Sherratt, Steven J. Sandler, and Kenneth J. Marians. "The Importance of Repairing Stalled Replication Forks." *Nature Reviews* 404 (2000): 37-41. Print.

7) Dose, K., A. Bieger-Dose, M. Labusch, and M. Gill. "Survival in Extreme Dryness and DNA-single-strand Breaks." *Advances in Space Research* 12.4 (1992): 221-29. Print.

8) Feng, Cui, Bharath Sunchu, Mallory E. Greenwood, and Matthew E. Lopper. "A Bacterial PriB with Weak Single-stranded DNA Binding Activity Can Stimulate the DNA Unwinding Activity of Its Cognate PriA Helicase." *BMC Microbiology* 189th ser. 11.1 (2011): 1-11. Print.

9) Harris, D. R., S. V. Pollock, E. A. Wood, R. J. Goiffon, A. J. Klingele, E. L. Cabot, W. Schackwitz, J. Martin, J. Eggington, T. J. Durfee, C. M. Middle, J. E. Norton, M. C. Popelars, H. Li, S. A. Klugman, L. L. Hamilton, L. B. Bane, L. A. Pennacchio, T. J. Albert, N. T. Perna, M. M. Cox, and J. R. Battista. "Directed Evolution of Ionizing Radiation Resistance in Escherichia Coli." *Journal of Bacteriology* 191.16 (2009): 5240-252. Print.

10) Heller, Ryan C., and Kenneth J. Marians. "Replication Fork Reactivation Downstream of a Blocked Nascent Leading Strand." *Nature* 439.7076 (2006): 557-62. Print.

11) Heller, Ryan C., and Kenneth J. Marians. "Replisome Assembly and the Direct Restart of Stalled Replication Forks." *Nature Reviews Molecular Cell Biology* 7.12 (2006): 932-43. Print.

12) Lohman, T. M., and K. P. Bjornson. "Mechanisms of Helicase-Catalyzed DNA Unwinding." *Annual Review of Biochemistry* 65.1 (1996): 169-214. Print.

13) Makarova, K. S., L. Aravind, Y. I. Wolf, R. L. Tatusov, K. W. Minton, E. V. Koonin, and M. J. Daly. "Genome of the Extremely Radiation-Resistant Bacterium Deinococcus Radiodurans Viewed from the Perspective of Comparative Genomics." *Microbiology and Molecular Biology Reviews* 65.1 (2001): 44-79. Print.

14) Satoh, Katsuya, Masahiro Kikuchi, Abu M. Ishaque, Hirofumi Ohba, Mitsugu Yamada, Kouhei Tejima, Takefumi Onodera, and Issay Narumi. "The Role of Deinococcus Radiodurans RecFOR Proteins in Homologous Recombination." *DNA Repair* 11.4 (2012): 410-18. Print.

15) Schaeffer, Patrick, Madeleine Headlam, and Nicholas Dixon. "Protein−Protein Interactions in the Eubacterial Replisome." *IUBMB Life (International Union of Biochemistry and Molecular Biology: Life)* 57.1 (2005): 5-12. Print.

16) Sunchu, Bharath, Linda Berg, Hayley E. Ward, and Matthew E. Lopper. "Identification of a Small Molecule PriA Helicase Inhibitor." *Biochemistry* 51.51 (2012): 10137-0146. Print.

17) White, O *et al*. "Genome Sequence of the Radioresistant Bacterium Deinococcus Radiodurans R1." *Science* 286.5444 (1999): 1571-577. Print.